



Article

The Effects of Wind Erosion Depending on Cropping System and Tillage Method in a Semi-Arid Region

Caihong Yang ^{1,*}, Yanxiang Geng ¹, Xing Zhou Fu ¹, Jeffrey A. Coulter ² and Qiang Chai ^{3,*}

¹ Gansu Provincial Key Lab of Aridland Crop Science/College of Forestry, Gansu Agricultural University, Lanzhou 730070, China; gengyx@st.gsau.edu.cn (Y.G.); fuxz@st.gsau.edu.cn (X.Z.F.)

² Department of Agronomy and Plant Genetics, University of Minnesota, St. Paul, MN 55108, USA; cault077@umn.edu

³ Gansu Provincial Key Lab of Aridland Crop Science/College of Agronomy, Gansu Agricultural University, Lanzhou 730070, China

* Correspondence: Yangch@gsau.edu.cn (C.Y.); Chaiq@gsau.edu.cn (Q.C.);
Tel.: +86-931-7608-083 (C.Y.); +86-931-7603-751 (Q.C.)

Received: 25 March 2020; Accepted: 27 April 2020; Published: 20 May 2020



Abstract: Wind erosion is a major environmental problem in arid and semi-arid regions, where it has significant impacts on desertification and soil degradation. To understand the effects of cropping systems and tillage methods on the reduction of soil wind erosion, wind tunnel investigations were performed on soil samples from an irrigated field in an experiment conducted in semi-arid northwestern China in 2016–2018. Three cropping systems for annual spring wheat (*Triticum aestivum* L.)/maize (*Zea mays* L.) strip intercropping (W/M), a two-year wheat-winter rape-maize rotation (WRM), and a two-year wheat-maize rotation (WM) were each evaluated with two tillage methods (conventional tillage without wheat straw retention (CT) and no-tillage with 25–30 cm tall wheat straw (NT)). The mean rate of soil erosion by wind with NT was 18.9% to 36.2% less than that with CT. With increasing wind velocity, the rate of soil erosion by wind increased for both CT and NT but was faster with CT than NT. Soil wind erosion occurred with a wind velocity $\geq 14 \text{ m s}^{-1}$, and NT greatly decreased the rate of soil erosion when wind velocity exceeded 14 m s^{-1} . W/M, WRM, and WM with NT increased non-erodible aggregates by 53.7%, 53.7%, and 54.9% in 2017, and 51.3%, 49.6% and 44.6% in 2018, respectively, than conventional tillage. At a height of 0–20 cm, the rate of soil transport with CT decreased with increasing height. The volume of soil transport at a height of 0–4 cm and soil transport percentage at a height of 0–4 and 0–20 cm (Q_{0-4}/Q_{0-20}) with NT were less than with CT. These findings show that NT with cropping system intensification can be an effective strategy for resisting wind erosion in irrigated semi-arid regions, thereby reducing the negative environmental impacts of crop production.

Keywords: soil wind erosion; crop rotation; intercropping; no tillage; wind-sand flow structure

1. Introduction

Wind erosion is the wind-forced entrainment, transportation, and deposition of soil particles [1]. It causes devastating global environmental degradation through movement of fine nutrient-rich surface soil particles to waterbodies, air and other land, thereby decreasing cropland productivity and increasing the risk to human health [2–5]. Wind erosion also impairs soil properties such as structure, moisture content, and organic matter [6], and it is enhanced by lack of vegetation on the soil surface [7].

Wind erosion is responsible for widespread desertification and land degradation in arid and semi-arid regions of northern China [8]. The cold climates of these regions lead to seasonal change in soil properties and vegetation cover [9]. During late winter to early spring, wind erosion is prominent in these regions due to high winds and bare, loose surface soil [10]. Soil wind erosion from exposed

cropland can be effectively controlled by conservational tillage [11–13], which is a strategy for reducing the soil sensitivity to erosion [14]. Crop system intensification can increase vegetation cover on the soil surface, thereby reducing wind erosion. The effects of tillage method and vegetative cover on the susceptibility of soil to wind erosion are well documented [15], but there has been limited research on soil resistance to wind erosion when conservational tillage and crop rotation are integrated in semi-arid regions.

Soil surface conditions of cropland are an important aspect of studies related to wind erosion [16,17]. Most previous research has focused on the changes in soil erodibility as affected by soil protection and conservation practices [18,19]. Wind erosion is more frequent and extreme with conventional tillage and less vegetative cover [13,20], but the underlying mechanisms are unclear. An understanding of soil resistance to wind erosion as affected by the integration of cropping system intensification and tillage method is imperative for reducing wind erosion, thereby improving global food security and reducing environmental degradation. In this research, a field experiment was implemented to investigate the effects of cropping system intensification and tillage method on soil wind erosion rate, blown soil structure, and soil particle size distribution. Results from this study could serve as a foundation for innovation and the adoption of agronomic practices for controlling soil wind erosion in semi-arid irrigated regions.

2. Materials and Methods

2.1. Experimental Site

The field experiment was conducted in 2016–2018 at the Gansu Agricultural University Oasis Experiment Station (37°96' N, 102°64' E), located in the eastern part of the Hexi Corridor in northwestern China. In this area, the average yearly precipitation is <155 mm; however, potential evaporation is >2400 mm. Long-term mean annual wind speed at this site is 2.73 m s⁻¹, and strong winds (≥17 m s⁻¹) occur 20–40 d yr⁻¹, mainly during November through April. Soil at the experimental site is classified as an Aridisol, a kind of desert land filled with calcareous particles, with soil bulk density in the 0–110 cm soil depth averaging 1.40 g cm⁻³. Total nitrogen (N), available phosphorus (P), and organic matter content in the 0–40 cm soil layer are 0.78, 5.84, and 14.3 g kg⁻¹, respectively. At this site, long-term average annual sunshine duration is >3010 h, annual accumulated air temperature >10 °C is 2985 °C, and the mean annual frost-free period is 155 d, which is enough for one season crop but insufficient for two. Prior to this study, the experimental site had been in annual crop production with traditional farming practices for several decades, the soil surface is exposed for about 6 months from November to April under conventional planting mode. In addition, the climate becomes rather dry and strong windy days are frequent during these months. Therefore, blown sand and dust storms occur frequently after harvest of crops, especially in the spring, and the wind erosion that has occurred on this cropland is very serious.

2.2. Experimental Design and Crop Management

The previous crop prior to the experiment was exclusively maize. The study was conducted as a two-factorial experiment, in a randomized block design with three replications, with treatments applied to the same plots in every year. The factors included the arrangement of three cropping systems and two tillage methods. The three cropping systems were annual wheat/maize strip intercropping (W/M), a two-year wheat-winter rape-maize rotation (WRM), and a two-year wheat-maize rotation (WM) (Table 1). Plastic film was used to cover the maize strips, which were mulched with colorless plastic film of 140 cm wide, and this was laid out by hand over the plot where the width of plastic film covering on the maize strip surface was 120 cm. The two tillage methods were conventional tillage without wheat straw retention (CT) and no-tillage with 25–30 cm tall wheat straw (NT). For CT, plots were moldboard plowed to a depth of 30 cm in the spring, followed by shallow harrowing prior to planting wheat or maize. These same tillage methods were used after wheat harvest and prior to planting

winter rape in the WRM rotation. No-tillage plots received zero tillage throughout the experiment and retained 25–30 cm tall wheat straw after harvest of the wheat grain. All aboveground wheat residues were removed from the CT plots soon after harvesting the wheat grain, and all aboveground maize and winter rape residues were removed from both NT and CT plots soon after harvest of maize and winter rape grain. In wheat/maize intercropping, intercropped maize and wheat were alternated each year; the maize strips in the previous year were planted with wheat in the current year and vice versa.

Table 1. Description of cropping system and tillage method treatments.

Cropping System Abbreviation	Tillage Methods	Cropping Sequence		
		2016	2017	2018
W/M WRM WM	Conventional tillage without wheat straw retention (CT)	wheat/maize wheat-winter rape wheat	wheat/maize maize maize	wheat/maize wheat-winter rape wheat
W/M WRM WM	No tillage with 25–30 cm tall standing wheat straw (NT)	wheat/maize wheat-winter rape wheat	wheat/maize maize maize	wheat/maize wheat-winter rape wheat

The selected spring wheat, maize, and winter oilseed rape cultivars were ‘Yong-liang 4’, ‘Longyou 6’ and ‘Sheng-dan 16’, respectively. Each plot was 110 m² (10 m wide × 11 m long). In the wheat/maize intercropping system, wheat and maize were sown in an east-west row orientation in alternating 220 cm wide strips, with five pairs of strips in each plot. Wheat strips were 80 cm wide (six rows with a 12 cm inter-row distance) and maize strips were 140 cm wide (three rows with a 40 cm inter-row distance). There was a 30 cm wide gap between wheat and maize strips. With intercropping and sole cropping, wheat and maize were sown to 675,000 and 82,500 plants ha⁻¹, respectively, and oilseed rape was sown at 11 kg seeds ha⁻¹. N (urea) and P (diammonium phosphate) fertilizers were used to supply wheat, maize, and oilseed rape with 225, 360, and 150 kg N ha⁻¹, respectively, and 66, 158, and 50 kg P₂O₅ ha⁻¹, respectively. Each crop received the same rate of fertilizers in the intercropping and sole cropping systems. All N fertilizer for wheat and oilseed rape, and all P fertilizer for all crops was applied as basal fertilizer prior to sowing. For maize, 30% of the total N fertilizer was applied as basal fertilizer prior to sowing, and 60% and 10% of the total N fertilizer rate was top-dressed at the six leaf collar and kernel blister maize phenological stage, respectively. In each year, irrigation (120 mm) was applied to all plots in the early winter before soil freezing. Additional irrigation was applied using a drip pipe system in the experimental areas. The irrigation schedule and amount was consistent across years and based on conventional local practices.

2.3. Measurement Indices and Methods

2.3.1. Description of Soil Samples

Undisturbed soil samples (30 cm × 20 cm) were collected from the 0–10 cm soil layer in each plot after soil thawing in the spring of 2017 and 2018. The samples were taken in sample boxes made of five steel plates that included one underside board and four wallboards (one wallboard was detachable). Soil samples were collected according to the methods described by Zhang et al. [21], which involved (i) excavating surrounding soils to a depth in excess of 10 cm without disturbing the soil surface of the selected sample area, (ii) placing the sample box, with one wallboard detached, over the sample area and invaginating the soil into the box, and (iii) smoothing the side of the soil along the wallboards and enveloping the soil with the detachable wallboard. Soil samples were cushioned to avoid disturbance during transport and were carefully transported by truck from the experimental field to the wind tunnel laboratory. The gravimetric soil moisture content of these soil samples was about 5.0% of dry matter mass before wind tunnel testing.

After sowing in each spring, undisturbed soil samples were collected from the surface 5 cm of each plot using bevel-edged steel rings of 10 cm diameter to determine aggregate size distribution. Roots and debris from each sample were removed and the remaining soil was stored in plastic bags, then air dried. In the laboratory, the soil samples were sieved with an 8 mm-sieve, and stored at room temperature. Dried soil was separated using a soil aggregate analyzer (TTF-100, Shangyu Shun Dragon Co., Shaoxing, China), similar in principle to a wet sieving device. A modified wet sieving procedure was used to measure soil aggregate size distribution. This apparatus was designed to allow recovery of all particle fractions from individual soil samples and handle stacked sieves (18 cm diameter \times 31.5 mm height). Soil particle fraction and five aggregate size grades were collected from each plot: >5 , 2–5, 1–2, 0.5–1, 0.25–0.5, 0.1–0.25, and <0.1 mm diameter. The apparatus specifications for stroke length (4 cm), frequency (30 cycles min^{-1}), and oscillation time (15 min) were held constant. Sieving was done in triplicate for each sample. After testing, the material remaining on each sieve was placed on a Petri dish and dried at 105 °C for 24 h. Dried soil aggregates from each size grade were weighed to determine the percentage of non-erodible aggregates.

2.3.2. Wind Tunnel Tests

Wind tunnel tests were conducted in the straight line forced wind tunnel at the Key Laboratory of Desert and Desertification of the Cold and Arid Regions Environmental and Engineering Research Institute, Chinese Academy of Science, Shapotou, China. The total length of the blow-type, non-circulating wind tunnel was 37 m, and the working section was 21 m long, 1.2 m wide, and 1.2 m high. The cross section of this wind tunnel can produce a stable airflow field and free turbulent airflow. Its static pressure gradient in the axial direction is 0.005, and its airflow velocity uniformity is 1%. Wind velocity was measured by a pitot tube installed 0.6 m above the tunnel floor and can be controlled continuously from 2 to 30 m s^{-1} via the control panel [22].

A prepared sampling tray was placed in the middle of the experimental section of the wind tunnel and the soil surface was paralleled to the test section's floor. The threshold wind speed required to initiate soil erosion for each soil sample was measured, then each sample was blown by free stream wind speeds of 6, 10, 14, 18, 22 m s^{-1} , which are close to the maximum monthly average wind speed at the experimental site at 30 cm above the soil surface. Each sample was blown at the aforementioned wind velocities from lower to higher at durations of 15, 12, 10, 8, 5 min, respectively. The mass of soil loss was calculated by comparing the weight difference before and after each test run. Weight loss was converted into soil wind erosion rate ($\text{g m}^{-2} \text{min}^{-1}$) to signify the modulus of soil wind erosion.

The wind-driven sediment of each sample was trapped in a ladder-like slit passive sampler that was 20 cm high with 10 openings, each 2 cm high and 2 cm wide. During the test, the deposition chamber was located at the central point of the wind tunnel cross-section and its position was 1 m downward from the back edge of the sample tray in the working section. An electronic scale was used to weigh blown soil and calculate the mass of soil transported at different heights; thus, sediment flux ($\text{g m}^{-2} \text{s}^{-1}$) vertical profiles of blown soil at 0–20 cm above the tunnel floor were obtained. Since a very small amount of sediment was blown at low wind speed, sediments were collected once after being blown at the three lowest wind velocities (6, 10, and 14 m s^{-1}). Sediments were collected once after being blown at the two highest wind velocities (18 and 22 m s^{-1}).

2.4. Data Analysis

All data were analyzed at $p < 0.05$ by analysis of variance using SPSS 19.0 (SPSS Institute, Inc., Chicago, IL, USA). Treatment means were compared with Duncan's multiple range test at $p < 0.05$ using SPSS 19.0.

3. Results

3.1. Erodibility of the Soils by Wind

3.1.1. Soil Wind Erosion Rate

Average soil wind erosion rate at five wind velocities was significantly influenced by tillage method and the interaction between cropping system and tillage method in both years (Table 2). The average wind erosion rate for CT was $36.13 \text{ g m}^{-2} \text{ min}^{-1}$ in 2017 and $29.61 \text{ g m}^{-2} \text{ min}^{-1}$ in 2018, 55% and 46% greater than that with NT, respectively. In 2017, average wind erosion rate was least with NT applied to all three cropping systems, and was greatest with CT applied to W/M and WM. Additionally, there was no significant difference between W/M and WRM with CT. In 2018, there was no significant difference among cropping systems for either tillage method.

Table 2. Rates of soil wind erosion ($\text{g m}^{-2} \text{ min}^{-1}$) as affected by cropping system, tillage method, and wind velocity in 2017 and 2018.

Treatments	Wind Velocity (m s^{-1})											
	2017						2018					
	6	10	14	18	22	Average	6	10	14	18	22	Average
W/M	2.45	12.08	27.77	46.28	90.58	35.83	3.23	8.65	18.10	33.90	80.48	28.87
WRM	2.11	11.64	25.33	37.29	86.51	32.58	2.89	9.72	17.56	36.63	82.91	29.94
WM	2.56	13.14	32.01	50.02	102.17	39.98	2.89	10.28	17.37	37.29	82.33	30.03
W/M	3.38	8.42	15.35	27.13	58.43	22.54	2.46	6.07	7.35	24.71	61.16	20.35
WRM	2.56	6.64	14.57	23.01	57.67	20.89	2.67	6.67	8.67	29.75	50.49	19.65
WM	2.78	9.58	16.67	26.84	76.67	26.51	2.68	4.81	7.17	26.67	63.45	20.96
Cropping system (C)	NS	NS	NS	*	*	NS	NS	NS	*	*	NS	NS
Tillage method (T)	NS	*	**	**	**	**	NS	*	**	**	**	**
C × T	NS	*	*	*	*	*	NS	NS	*	*	*	*

NS, not significant at $p < 0.05$. * Significant at $p < 0.05$. ** Significant at $p < 0.01$.

Soil wind erosion rate was not significantly affected by the cropping system or tillage method at a wind velocity of 6 m s^{-1} in either year (Table 2). Across treatments, the wind erosion rate at a wind velocity of 6 m s^{-1} averaged $2.64 \text{ g m}^{-2} \text{ min}^{-1}$ in 2017 and $2.80 \text{ g m}^{-2} \text{ min}^{-1}$ in 2018. Soil wind erosion rate was significantly influenced by the interaction between the cropping system and tillage method at wind velocities of 14, 18, and 22 m s^{-1} in both years and at a wind velocity of 10 m s^{-1} in 2017 (Table 2). Additionally, tillage method significantly affected soil wind erosion rate at a wind velocity of 10 m s^{-1} in 2018. At a wind velocity of 10 m s^{-1} , the rate of soil wind erosion in 2017 was greatest with CT and all cropping systems (mean = $12.29 \text{ g m}^{-2} \text{ min}^{-1}$) and least with NT applied to WRM ($6.64 \text{ g m}^{-2} \text{ min}^{-1}$). In 2018, soil wind erosion rate was not significantly influenced by cropping system but was significantly greater with CT than NT (9.55 and $5.85 \text{ g m}^{-2} \text{ min}^{-1}$, respectively). In 2017, the rate of soil wind erosion at wind velocities of 14 and 18 m s^{-1} was greatest with CT and WM, and least with NT applied to all three cropping systems. At a wind velocity of 22 m s^{-1} in 2017, the rate of soil wind erosion was also greatest with CT and WM, and was least when NT was applied to W/M and WRM. In 2018, the rate of soil wind erosion was greatest with CT applied to all three cropping systems at wind velocities of 14 and 22 m s^{-1} , and with CT applied to WRM at a wind velocity of 18 m s^{-1} . In 2018, the rate of soil wind erosion was minimized when NT was applied to all three cropping systems at a wind velocity of 14 m s^{-1} , W/M and WM at a wind velocity of 18 m s^{-1} , and WRM at a wind velocity of 22 m s^{-1} .

3.1.2. Relationship between Soil Erosion Rate and Wind Velocity

The rate of soil wind erosion increased by a power function with increasing wind velocities for all pairs of cropping system and tillage method, and was greater with CT than NT (Table 3). There are also differences among cropping systems. With NT, the rate of increase in soil wind erosion with increased wind velocity was $W/M < WRM < WM$ in 2017, and $WRM < W/M < WM$ in 2018.

Table 3. Relationship between wind-blown soil mass and wind speed as affected by cropping system in 2017 and 2018.

Treatment	Regression Equation	Correlation Coefficient
W/M	$Q = 0.0291v^{2.5436}$	0.995
WRM CT	$Q = 0.0247v^{2.5884}$	0.991
WM	$Q = 0.0256v^{2.6181}$	0.995
W/M	$Q = 1.0057e^{0.1828v}$	0.991
WRM NT	$Q = 0.9158e^{0.1859v}$	0.996
WM	$Q = 0.8756e^{0.1951v}$	0.991

Q , Rate of soil wind erosion; v , wind velocity.

3.2. Soil Aggregates

3.2.1. Non-Erodible Aggregates

For soil aggregates in the surface layer (0–5 cm), the amount of non-erodible aggregates (>1 mm diameter) with NT was significantly greater than that with CT (Figure 1). Compared with corresponding conventional tillage, W/M, WRM, and WM increased non-erodible aggregates by 53.72%, 53.73%, and 54.89% in 2017, and 51.33%, 49.60% and 44.64% in 2018, respectively. There were significant differences between NT and CT at all the tested wind velocities ($p < 0.05$).

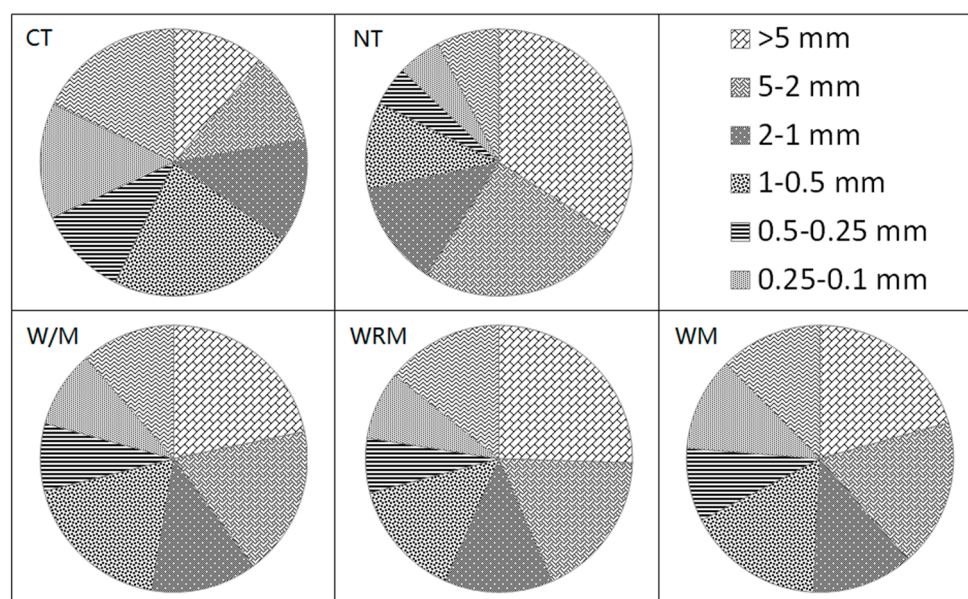


Figure 1. Percentage of soil aggregates under in different diameter classes within the 0–5 cm soil layer, as affected by cropping system and tillage method during two years.

3.2.2. Relationship between Non-Erodible Aggregates and Wind Velocity

Soil protection was mainly provided by wheat residues, winter rape coverage and plastic mulch in maize. Soil resistance to wind erosion was mainly due to wet-measured, non-erodible aggregates with NT applied to WRM. This difference can be explained by soil protection by residues from previous crops and mulch in maize. Linear correlation was used to fit non-erodible aggregates in topsoil (0–5 cm) to the soil wind erosion rate at a wind velocity of 22 m s^{-1} . There was a negative linear correlation between non-erodible aggregates and rate of soil wind erosion at a wind velocity of 22 m s^{-1} (Figure 2).

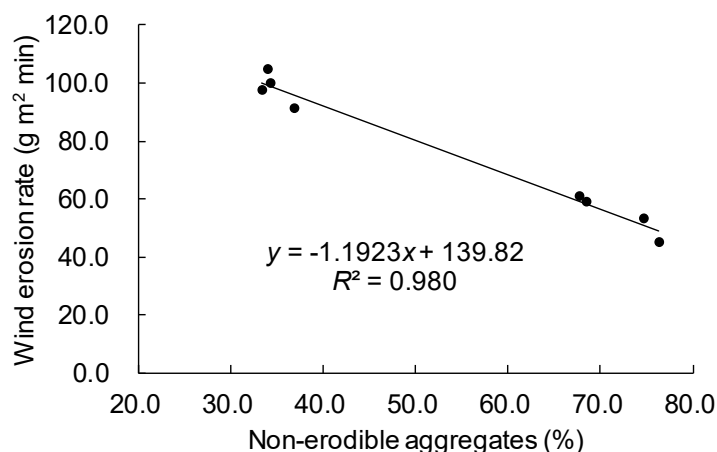


Figure 2. Relationship between soil wind erosion rate and percent mass of non-erodible soil particles, across cropping systems and tillage methods during two years.

3.3. Mass Flux Vertical Profile of Blown Soil

Based on analysis of the percentage of soil transport at a height of 0–20 cm (Figure 3), there were large differences in the vertical mass flux profile of blown soil as affected by cropping system and tillage method. The total mass of soil transported with CT was about two to four times greater than that with NT at a height of 0–20 cm, but the differences among cropping systems with NT were no more than 20.7% in 2017 and 22.4% in 2018. The ratio of mass of soil transported at a height of 0–4 cm and total mass of soil transported at a height of 0–20 cm (Q_{0-4}/Q_{0-20}) for CT ranged from 45% to 50% at the various wind velocities, but was $\leq 42\%$ with NT.

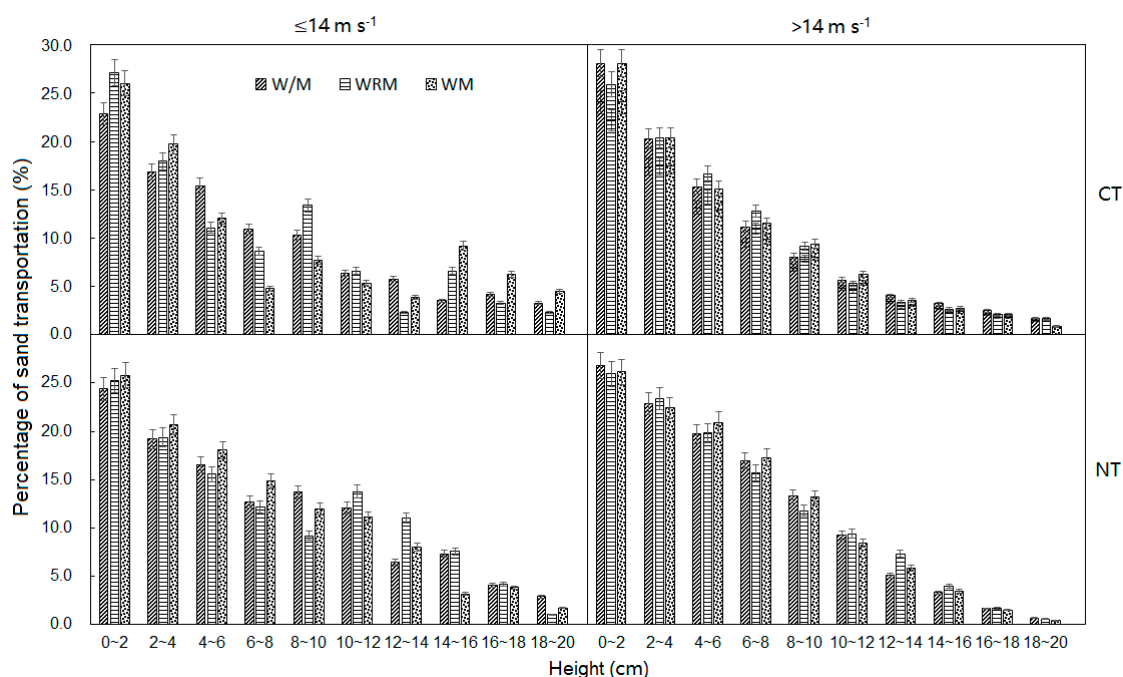


Figure 3. Percentage of sand transportation as affected by cropping system, tillage method, and wind velocity and height during two years. Note: CT, conventional tillage without wheat straw retention; NT, no-tillage with 25–30 cm tall wheat straw; W/M, annual wheat/maize strip intercropping; WRM, two-year wheat-winter rape-maize rotation; WM, two-year wheat-maize rotation. Error bars are standard errors of the means.

Soil mass flux was mainly concentrated in airflow near the soil surface with both NT and CT. The disparity of Q_{0-4}/Q_{0-20} between CT and NT increased with increasing wind velocity. Compared with CT, the total amount of sand transported at a height of 0–20 cm and the fraction of sand transported at a height of 0–4 cm decreased with NT. Across years and cropping systems, the difference between tillage systems ranged from 3.71% to 17.65% at a wind velocity of 18 m s^{-1} and from 6.15% to 24.55% at a wind velocity of 22 m s^{-1} . The Q_{0-4}/Q_{0-20} was also significantly affected by cropping system. No-tillage decreased the percentage of soil transport with increasing height for all cropping systems, and these gradients of decline were greater than those with CT. The ratio of mass of soil transported at a height of 0–10 cm and total mass of soil transported at a height of 10–20 cm (Q_{0-10}/Q_{10-20}) among cropping systems with CT ranged from 0.77–0.87 in 2017 and 0.74–0.85 in 2018. Differences in Q_{0-10}/Q_{10-20} among cropping systems with NT decreased by 5.24% in 2017 and 9.22% in 2018 with increasing wind velocity. Additionally, Q_{0-4}/Q_{0-20} decreased with increasing wind velocity but Q_{10-20}/Q_{0-20} increased with different cropping systems and tillage methods.

Quantitative relationships between the percentage of soil transport and height were established from the study results of the vertical mass flux profile of blown soil (Table 4). The results show that the soil transport rate decreased with increasing height for all combinations of cropping system and tillage method, and that the extent of the reduction with NT was less than that with CT. At a height of 0–20 cm, the percentage of soil transport with CT significantly decreased with increasing height by a negative exponent, whereas a significant negative linear relationship existed for NT in both years. Therefore, the rate of decrease in soil transport rate with increasing height was less with NT than CT.

Table 4. Relationship between sand transport rate (S) and above the soil surface (H) as affected by cropping system, tillage method, and wind velocity during two years.

Treatments	Wind Velocity ($\text{m}\cdot\text{s}^{-1}$)			
	18		22	
	Regression Equation	Correlation Coefficient	Regression Equation	Correlation Coefficient
W/M	$S = 0.0213e^{-0.131H}$	0.988	$S = 0.0452e^{-0.18H}$	0.997
WRM	$S = 0.0216e^{-0.157H}$	0.985	$S = 0.0399e^{-0.188H}$	0.973
WM	$S = 0.0276e^{-0.158H}$	0.975	$S = 0.0382e^{-0.208H}$	0.969
W/M	$S = -0.0005H + 0.0086$	0.982	$S = -0.0006H + 0.0105$	0.970
WRM	$S = -0.0003H + 0.0066$	0.993	$S = -0.0005H + 0.0099$	0.965
WM	$S = -0.0006H + 0.0104$	0.970	$S = -0.0007H + 0.0128$	0.967

4. Discussion

Soil erosion occurs when the wind speed exceeds a certain threshold value (threshold shear velocity), which is enough to overcome the resistance of soil aggregates to detachment [1]. The threshold wind velocity depends on a number of factors including field surface conditions, surface roughness, shape and size of the soil aggregates, content of soil clay particles, and near surface soil water content [23,24]. In this study, NT decreased the surface soil loss due to wind erosion at various wind velocities and the amount of sand transported at a certain height above soil surface, especially with WRM and NT. Meanwhile, soil aggregates with NT influenced the degree of differentiation among cropping systems. Strong winds with speeds $>14 \text{ m s}^{-1}$ gave rise to soil wind erosion in this semi-arid region of northwestern China, similar to the results reported in other research [22,25,26]. The findings of previous studies of wind tunnel experiments showed that soil wind erosion rate was intensified significantly with increasing wind velocities by a power function [27,28]. Soil wind erosion rates increased faster with increasing wind velocities under the bigger of the exponentials. In this study, we found that soil wind erosion rate increased by a power function with increasing wind velocity for all combinations of cropping system and tillage method, but the exponential of the power function was far greater with CT than NT.

The profile of wind-transported sand grains versus height, which is described by the concentration or mass flux [29]. It reflects the distribution of sand transport rate on the vertical profile above the ground, which has direct effects on the sand transport rate. This research showed that the percentage of sand transportation decreased with increasing height, which is consistent with the finding of Liu et al. [26]. Additionally, the extent of the reduction under NT was smaller than with CT. Compared with conventional tillage, the total amount of sand transported at the height of 0–20 cm and the fraction of sand transported at the height of 0–4 cm were decreased under conservational tillage. Among the combinations of cropping system and tillage method evaluated in this study, WRM with NT was most effective, as it increased the coverage of the soil surface, improved soil aggregation, and reduced the magnitude of the vertical mass flux profile of blown soil near the field surface.

The aforementioned results indicate that soil wind erosion is generally more serious with CT compared to NT, and that the difference is magnified with cropping system intensification. As mentioned above, surface non-erodible soil aggregates increased with WRM and NT due to the cohesion of soil particles, which can greatly reduce soil wind erosion [18]. In the long term, cropland soil properties can improve over time with the use of conservation tillage and coverage of the soil surface, which may contribute to reduced soil wind erosion [30]. Among the combinations of cropping system and tillage method in this study, the order of soil wind erosion rate was WM (CT) > W/M (CT) > WRM (CT) > WM (NT) > W/M (NT) > WRM (NT) over a two year period and the order of Q_{0-4}/Q_{0-20} was WM (CT) > WRM (CT) > W/M (CT) > WRM (NT) > W/M (NT) > WM (NT) in 2017 and W/M (CT) > WM (CT) > WRM (CT) > WM (NT) > W/M (NT) > WRM (NT) in 2018. The results from this study support the hypothesis that cropping system intensification with NT can improve wind erosion control in semi-arid regions where wind erosion is common. The intensified WRM with NT significantly decreased the amount of sand transported near the field surface at high wind velocities and the rate of soil wind erosion on irrigated cropland in a semi-arid region. Future research should address additional strategies for cropping system intensification (e.g., cover crops) with NT and additional conservation tillage methods to identify additional strategies for controlling soil wind erosion.

5. Conclusions

In this research, the effects of cropping system intensification and tillage method on soil wind erosion was evaluated with wind tunnel experiments. The mean rate of soil wind erosion with NT was 18.92% to 36.15% less than that with CT. A power function described the relationship between the rate of wind erosion and wind velocity for six simulated combinations of cropping system and tillage method, and the rate of increase in wind with increasing wind velocity was greater with CT than NT. Soil wind erosion was significantly aggravated when the wind velocity reached 14 m s^{-1} or more, and NT greatly decreased the rate of wind erosion when the wind velocity was $>14 \text{ m s}^{-1}$.

Non-erodible soil aggregates ($>1 \text{ mm}$ diameter) with NT were greater than those with CT on account of stronger cohesion of soil particles and larger aggregates that are more difficult to erode. The WRM with NT increased non-erodible aggregates; that is, the protective cover of crop residues with this intensified cropping system prevented soil particles from being transported and increased the quantity and size of soil aggregates in the 0–5 cm soil layer, which can partly control wind erosion.

At a height of 0–20 cm, the soil transport rate decreased with increasing height by a linear function with CT and an exponential function with NT. The total volume of soil transport at a height of 0–4 cm and Q_{0-4}/Q_{0-20} with NT were less than that with CT. The results indicate that less tillage coupled with cropping system intensification (WRM) is a useful approach for reducing wind erosion of irrigated cropland in semi-arid regions where high winds and desertification threaten agricultural and environmental sustainability. Future research should investigate additional strategies for cropping system intensification (e.g., cover crops and relay cropping) and soil coverage (i.e., mulching) with NT and other methods of conservation tillage to develop more options for controlling soil wind erosion.

Author Contributions: Q.C. conceived and designed the experiments; Y.G., X.Z.F., and C.Y. performed the experiments; C.Y. and J.A.C. analyzed the data and wrote the paper; J.A.C. assisted with writing, reviewing and editing the paper. All authors have read and agreed to the published version of the manuscript.

Funding: This research was sponsored by Gansu Provincial Key Laboratory of Aridland Crop Science of Gansu Agricultural University (GSCS-2019-6), National Ten Thousand Talents Program, the Discipline Construction Fund Project of Gansu Agricultural University (GSAU-XKJS-2018-106), the National Natural Science Foundation of China (41561062, 31771738), the Natural Science Foundation of Gansu Province of China (18JR3RA176), and the Modern Agriculture Green Manure Industry Technology System (CARS-22-G-12).

Acknowledgments: The authors would like to thank the staff at the Gansu Agricultural University Oasis Experiment Station for their assistance to the workshops, Yan-Xiang Geng, Jun-Qiang Wang, Xing-Zhou Fu, Chang-Geng Yan and Yu-Hao Zhao for their contributions to the experiment, and some peer reviewers for their comments on the manuscript.

Conflicts of Interest: The authors declare that they have no conflict of interest.

References

1. Ravi, S.; Zobeck, T.M.; Over, T.M.; Okin, G.S.; D’Odorico, P. On the effect of moisture bonding forces in air-dry soils on threshold friction velocity of wind erosion. *Sedimentology* **2006**, *53*, 597–609. [[CrossRef](#)]
2. Foltz, G.R.; McPhaden, M.J. Impact of Saharan Dust on Tropical North Atlantic SST. *J. Clim.* **2008**, *21*, 5048–5060. [[CrossRef](#)]
3. Soukup, D.; Buck, B.; Goossens, D.; Ulery, A.; McLaurin, B.T.; Baron, D.; Teng, Y.X. Arsenic concentrations in dust emissions from wind erosion and off-road vehicles in the Nellis Dunes Recreational Area, Nevada, USA. *Aeolian Res.* **2012**, *5*, 77–89. [[CrossRef](#)]
4. Santra, P.; Moharana, P.C.; Kumar, M.; Soni, M.L.; Pandey, C.B.; Chaudhari, S.K.; Sikka, A.K. Crop production and economic loss due to wind erosion in hot arid ecosystem of India. *Aeolian Res.* **2017**, *28*, 71–82. [[CrossRef](#)]
5. Zhang, H.Y.; Fan, J.W.; Cao, W.; Harris, W.; Li, Y.Z.; Chi, W.Y.; Wang, S.Z. Response of wind erosion dynamics to climate change and human activity in Inner Mongolia, China during 1990 to 2015. *Sci. Total Environ.* **2018**, *639*, 1038–1050. [[CrossRef](#)] [[PubMed](#)]
6. Zobeck, T.M.; Baddock, M.; Scott, V.P.R.; Tatarko, J.; Acosta-Martinez, V. Soil property effects on wind erosion of organic soils. *Aeolian Res.* **2013**, *10*, 43–51. [[CrossRef](#)]
7. Borrelli, P.; Ballabio, C.; Panagos, P.; Montanarella, L. Wind erosion susceptibility of European soils. *Geoderma* **2014**, *232–234*, 471–478. [[CrossRef](#)]
8. Wang, X.; Wang, T.; Dong, Z.; Liu, X.; Qian, G. Nebkha development and its significance to wind erosion and land degradation in semi-arid northern China. *J. Arid Environ.* **2006**, *65*, 129–141. [[CrossRef](#)]
9. Tang, Z.G.; Ma, J.H.; Peng, H.H.; Wang, S.H.; Wei, J.F. Spatiotemporal changes of vegetation and their responses to temperature and precipitation in upper Shiyang river basin. *Adv. Space Res.* **2017**, *60*, 969–979. [[CrossRef](#)]
10. Li, F.R.; Zhao, L.Y.; Zhang, H.; Zhang, T.H.; Shirato, Y. Wind erosion and airborne dust deposition in farmland during spring in the Horqin Sandy Land of eastern Inner Mongolia, China. *Soil Tillage Res.* **2004**, *75*, 121–130. [[CrossRef](#)]
11. Jia, H.L.; Gang, W.; Guo, L.; Zhuang, J.; Tang, L. Wind erosion control utilizing standing corn residue in Northeast China. *Soil Tillage Res.* **2015**, *153*, 112–119. [[CrossRef](#)]
12. Pelt, R.S.V.; Hushmurodov, S.X.; Baumhardt, R.L.; Chappell, P.; Nearing, M.A.; Polyakov, V.O.; Strack, J.E. The reduction of partitioned wind and water erosion by conservation agriculture. *Catena* **2017**, *148*, 160–167. [[CrossRef](#)]
13. Singh, P.; Sharratt, B.; Schillinger, W.F. Wind erosion and PM10 emission affected by tillage systems in the world’s driest rainfed wheat region. *Soil Tillage Res.* **2012**, *124*, 219–225. [[CrossRef](#)]
14. Schlatter, D.C.; Schillinger, W.F.; Bary, A.I.; Sharratt, B.; Paulitz, T.C. Dust-associated microbiomes from dryland wheat fields differ with tillage practice and biosolids application. *Atmos. Environ.* **2018**, *185*, 29–40. [[CrossRef](#)]
15. Mendez, M.J.; Buschiazzo, D.E. Soil coverage evolution and wind erosion risk on summer crops under contrasting tillage systems. *Aeolian Res.* **2015**, *16*, 117–124. [[CrossRef](#)]

16. Liu, L.; Zhang, Z.D.; Zhang, K.L.; Liu, H.Y.; Fu, S.H. Magnetic susceptibility characteristics of surface soils in the Xilingele grassland and their implication for soil redistribution in wind-dominated landscapes: A preliminary study. *Catena* **2018**, *163*, 33–41. [[CrossRef](#)]
17. Oro, L.A.D.; Colazo, J.C.; Buschiazzo, D.E. RWEQ–Wind erosion predictions for variable soil roughness conditions. *Aeolian Res.* **2016**, *20*, 139–146. [[CrossRef](#)]
18. Wang, L.; Shi, Z.H.; Wu, G.L.; Fang, N.F. Freeze/thaw and soil moisture effects on wind erosion. *Geomorphology* **2014**, *207*, 141–148. [[CrossRef](#)]
19. Webb, N.P.; Strong, C.L. Soil erodibility dynamics and its representation for wind erosion and dust emission models. *Aeolian Res.* **2012**, *3*, 165–179. [[CrossRef](#)]
20. Pi, H.; Sharratt, B.; Schillinger, W.F.; Bary, A.L.; Cogger, C.G. Wind erosion potential of a winter wheat–summer fallow rotation after land application of biosolids. *Aeolian Res.* **2018**, *32*, 53–59. [[CrossRef](#)]
21. Zhang, C.L.; Zou, X.Y.; Yang, P.; Dong, Y.X.; Li, S.; Wei, X.H.; Yang, S.; Pan, X.H. Wind tunnel test and ¹³⁷Cs tracing study on wind erosion of several soils in Tibet. *Soil Tillage Res.* **2007**, *94*, 269–282. [[CrossRef](#)]
22. Dong, Z.B.; Liu, X.P.; Wang, H.T.; Zhao, A.G.; Wang, X.M. The flux profile of a blowing sand cloud: A wind tunnel investigation. *Geomorphology* **2003**, *49*, 219–230. [[CrossRef](#)]
23. Chepil, W.S.; Milne, R.A. Wind erosion of soil in relation to roughness of surface. *Soil Sci.* **1941**, *52*, 417–433. [[CrossRef](#)]
24. Li, J.R.; Flagg, C.; Okin, G.S.; Painter, T.H.; Dintwe, K.; Belnap, J. On the prediction of threshold friction velocity of wind erosion using soil reflectance spectroscopy. *Aeolian Res.* **2015**, *19*, 129–136. [[CrossRef](#)]
25. Chen, Z.; Cui, H.M.; Wu, P.; Sun, Y.C. Study on the optimal intercropping width to control wind erosion in North China. *Soil Tillage Res.* **2010**, *110*, 230–235. [[CrossRef](#)]
26. Liu, M.X.; Wang, J.A.; Yan, P.; Liu, L.Y.; Ge, Y.Q.; Li, X.Y.; Hu, X.; Yang, S.; Wang, L. Wind tunnel simulation of ridge-tillage effects on soil erosion from cropland. *Soil Tillage Res.* **2006**, *90*, 242–249. [[CrossRef](#)]
27. Xie, S.B.; Qu, J.J.; Wang, T. Wind tunnel simulation of the effects of freeze-thaw cycles on soil erosion in the Qinghai-Tibet Plateau. *Sci. Cold Arid Reg.* **2016**, *8*, 187–195.
28. Zamani, S.; Mahmoodabadi, M. Effect of particle-size distribution on wind erosion rate and soil erodibility. *Arch. Agron. Soil Sci.* **2013**, *59*, 1743–1753. [[CrossRef](#)]
29. Zheng, X.J.; He, L.H.; Wu, J.J. Vertical profiles of mass flux for windblown sand movement at steady state. *J. Geophys. Res. Solid Earth.* **2004**, *109*, B01106. [[CrossRef](#)]
30. Tanner, S.; Katra, I.; Argaman, E.; Ben-Hur, M. Erodibility of waste (Loess) soils from construction sites under water and wind erosional forces. *Sci. Total Environ.* **2018**, *616–617*, 1524–1532. [[CrossRef](#)]



© 2020 by the authors. Licensee MDPI, Basel, Switzerland. This article is an open access article distributed under the terms and conditions of the Creative Commons Attribution (CC BY) license (<http://creativecommons.org/licenses/by/4.0/>).